AN ANALYSIS OF RECENT FUEL-DISRUPTION EXPERIMENTS

CONF-820704--37

J. M. Kramer, T. E. Kraft, R. J. DiMelfi,
G. R. Fenske, and E. E. Gruber

Argonne National Laboratory
Argonne, Illinois 60439, U.S.A.

DE83 008467

ABSTRACT

Recent USDOE-sponsored DEH, FGR, and TREAT F series fuel-disruption experiments are analyzed with existing analytical models. The experiments are interpreted and the results used to evaluate the models. Calculations are presented using the FRAS3 fission-gas-behavior code and the DiMelfi-Deitrich fuel-response model.

INTRODUCTION

Early fuel dispersal in a hypothetical LMFBR loss-of-flow (LOF) accident is a potential mechanism for mitigation of accident energetics [1]. This dispersal is the result of a complex series of processes starting with the disruption of the fuel geometry and ending with the axial displacement of the fuel under the influence of gravity and hydrodynamic forces. Retained fission gases play a key role in early fuel dispersal since they influence both the time of fuel disruption and the character of disrupted fuel as well as providing a potentially substantial driving force for axial fuel motion. Furthermore, even in cases where early fuel dispersal does not occur, it may be possible for retained fission gas to significantly retard the collapse of the fuel under gravitational forces. Important factors that influence fuel behavior under LOF conditions include the fuel and cladding thermal history (temperature, temperature gradient, melting), the fuel microstructure, fuel deformation and cracking, fission product release and swelling, and cladding constraint on the fuel prior to disruption.

Both in-reactor and out-of-reactor experiments have been performed to provide phenomenological data on fuel disruption and fission gas behavior under LOF conditions. The most recent USDOE-sponsored in-reactor experiments are Argonne National Laboratory TREAT tests F3 and F4 [2]. Out-of-reactor experiments which have recently been completed include the DEH-I [3] and -IC [4] series of Direct Electrical Heating experiments performed at Argonne National Laboratory and new FGR [5] Fission Gas Release experiments performed at Hanford Engineering Development Laboratory.

Contributing to the understanding of fuel disruption and fission gas behavior are two analytical models developed at Argonne National Laboratory. The two models are: (a) the FRAS3 code [6,7,8], which models the detailed time-dependent formation and behavior of intragranular and intergranular fission-gas bubbles and their effect on the solid fuel; and (b) the DiMelfi-Deitrich (D-D) model [9,10] of grain-boundary gas pressurization and pressure relief during transient heating.

MASTER

The purpose of the work presented here was to systematically compare the results predicted by the current version of the FRAS3 code and by the D-D model with results from the recent fuel disruption experiments. In using these models in this study, no extraordinary attempt was made to calibrate the models to fit the data or to modify the experiment conditions from those reported by the experimenters. In some cases this has precluded the often cherished "excellent agreement," but it did allow the models to be evaluated and has led to the correction of some model deficiencies.

DESCRIPTION OF THE MODELS

Because a discussion of the analysis made in this study requires an understanding of the models and their underlying assumptions, it is necessary to give a brief, qualitative description of the two analytical tools which were used.

The FRAS3 Code

The FRAS3 [6,7,8] code is a structured collection of models of various aspects of transient fission-gas behavior in oxide fuel. The basis of the calculation is the Gruber model of bubble migration by surface diffusion within the fuel grain. The diffusion coefficient for the bubble is determined from the surface-diffusion coefficient with the mobility of very small bubbles limited because of the reduced effectiveness of the mass-transport mechanism. The evolution of the bubble-size disribution, with discrete size classes characterized by the number of gas atoms per bubble, is calculated from the coalescence probability. It is assumed that two bubbles coalesce instantly, conserving volume, if they touch. Coalescence probabilities are determined for random bubble migration and for biased migration in a thermal gradient. When two bubbles coalesce the gas pressure in the product bubble is in general not in equilibrium with the surface tension and external pressure constraints. The mean radius of bubbles in each size class is then calculated in FRAS3 to increase toward equilibrium at a rate controlled by vacancy transport to the bubbles.

Thermally biased migration of bubbles by surface diffusion is also assumed to be an important means by which fission gas reaches the grain boundaries. In calculating the escape of intragranular gas bubbles, the grains are approximated by spheres, and bubble diffusion across the boundaries is calculated from both random migration and average-velocity biased migration. Grain-boundary bubble populations are calculated by considering all bubbles arriving at the grain boundary in a given transient time step to have the current mean size. Coalescence of these intragranular bubbles with existing boundary bubbles is calculated, as well as coalescence between grain-boundary bubbles via migration in a thermal gradient. The grain-boundary bubbles are assumed to equilibrate instantaneously upon coalescence.

Grain-edge porosity is modeled as a simple network of straight, cylindrical tunnels. When the grain-boundary bubble population exceeds a concentration corresponding to an areal coverage of 50%, the excess gas is assumed to be transported to the edge tunnels. The equilibrium tunnel diameter is calculated and used to predict edge swelling. When the tunnel diameter reaches a limit corresponding to 5% of the fuel volume, the expansion is halted. This value of edge swelling was chosen to approximate the level at which the grain-edge porosity becomes stably interconnected. Further addition of gas from the boundaries is assumed to increase the grain-edge gas pressure, providing a driving force for expulsion of gas from the fuel through interlinked porosity and cracks. This expulsion is not calculated in the FRAS3 code, which provides only a single-node analysis.

The input values required by the version of FRAS3 used in this study are the volumetric gas-atom concentration, the fuel-grain size, and the time-dependent temperature and temperature gradient. Diffusion-coefficient parameters are also input, but these do not change from test to test. The gas atoms are assumed to be uniformly distributed in solution in the grains; initially no gas is on the grain boundaries and no gas bubbles exist.

Among the results obtained from FRAS3 are: fuel swelling due to fission gas within grains, on grain boundaries, and in grain-edge tunnels; the gas distribution in these same categories, from which localized gas release can be inferred; and various observable parameters, such as mean bubble sizes within grains and on grain boundaries, as well as the complete intragranular and intergranular bubble-size distributions.

Recent improvements to FRAS3 include an explicit model for grain-boundary bubble equilibration [7,8] and a capability for inputing an initial bubble distribution into the code. These improvements are part of a developmental version of FRAS3 and were not used for the calculations presented here.

The DiMelfi-Deitrich (D-D Model)

The response of grain-boundary bubbles to thermal transients and the resulting effect on overall transient fuel behavior is addressed by the D-D model [9,10]. The model is used to characterize the gross fuel behavior mode as a function of time. Brittle behavior is associated with rapid venting of gas to grain edges without significant grain-boundary swelling. This mode is a consequence of the tendency of bubbles to act as nuclei of unstable cracks that propagate in the grain-boundary during transients. Ductile behavior is associated with rapid grain-boundary swelling and occurs when the bubbles quickly achieve their equilibrium volume by mass transport.

The model is based on the concept that a grain-boundary bubble can expand and reduce the gas pressure either by propagating as a narrow crack in the grain boundary or by expansion as a bubble via vacancy diffusion. The former behavior contributes much less to volumetric swelling than the latter. By comparing the rates at which these two processes occur, a condition is derived for the onset of ductile behavior. This condition prevails when the grain-boundary diffusion coefficient exceeds a calculated minimum value for which the rates of expansion by the two processes are equal. Both this minimum value and the grain-boundary diffusion coefficient vary throughout the transient, but when the condition is met, rapid bubble equilibration and grain-boundary swelling are predicted to occur.

The D-D model involves a single adjustable parameter that theoretically depends on the grain-boundary bubble geometry. In practice, the parameter is fixed for one pair of transient experiments and its value calculated by extrapolation for other experiments. The extrapolation variable is the amount of fission gas retained after steady state irradiation. A single value of this parameter is applicable both to the first stage of dual-ramp tests and to single-ramp tests for a given fuel; but because exposure to the first stage of a dual-ramp test alters the bubble morphology, this parameter must be re-evaluated for the second stage.

Application of the model to a particular experiment provides the threshold time for swelling, which is determined from the time in the transient when the condition is met for ductile behavior. This threshold time can be compared directly to the time at which gross radial swelling is observed in the experiments.

Recently, the concepts embodied in the D-D model have been extended [10] to quantify the experimentally observed solid-fuel fragmentation during the early

stages of simulated LOF transients. In this model it is assumed that fission gas bubbles on grain boundaries in the fuel are in equilibrium subjected to a compressive constraining force maintained by the presence of intact cladding. When the constraining force is removed at cladding failure, the bubbles are overpressurized. If the overpressure is calculated to be sufficient to fracture the grain boundaries, the fission gas is assumed to expand to the ambient pressure with the work done being converted into kinetic energy of the fuel fragments. The overall fission gas content and its radial profile are considered in the calculations. Results from these calculations include the extent of fuel fragmentation, average particle size, and average particle velocity.

DESCRIPTION OF EXPERIMENTS

The experimental data used in the study are derived from USDOE-sponsored programs at Argonne National Laboratory (ANL) and Hanford Engineering Development Laboratory (HEDL). The ANL tests considered are from the out-of-reactor Direct Electrical Heating (DEH) experiments and the in-reactor TREAT F series experiments. The HEDL tests considered are from the Fission Gas Release (FGR) experiments. A brief description of the experiment objectives, apparatus, and test parameters is given below.

Direct Electrical Heating I-Series and IC-Series Tests

The DEH apparatus consists of an in-cell helium-filled chamber in which a fuel sample is placed with electrodes connected at the ends. A controlled electrical current is passed through the fuel stack resulting in ohmic heating. The feature distinguishing the tests in this study from previous DEH tests is the addition of a tungsten wire-mesh external heater surrounding the stack. The external heater was devised to reduce the large, non-prototypic temperature gradient in the fuel in previous DEH tests. In addition, in the IC series tests the heaters permitted the testing of stainless steel clad fuel samples by allowing the cladding to be melted off prior to ohmic heating of the fuel.

The I series tests analyzed here are I-35, I-37 through I-45, I-48, and I-49 [3]. The fuel element samples came from HEDL N-E pins preirradiated to ~2.5 at.% burnup at a peak power of ~40 kW/m. Because the steel cladding will short the DEH electrodes, the fuel pellets in these tests were extruded from the cladding into quartz tubes. In all but two tests the extruded stacks were used without further conditioning. In I-48 and I-49 the stack was heated to 1300°C for ten minutes prior to the transient to anneal the fuel.

In most DEH experiments the external heater and ohmic heating currents are controlled to simulate the initiating phase of a hypothetical loss-of-flow accident in a breeder reactor. These simulations comprise an initial slow temperature ramp (~30 K/s, average) for ~10 s corresponding to the postulated coolant flow coastdown and a secondary faster ramp (>100 K/s) corresponding to the period of sodium voiding. The experiments terminate either at a preset interruption in power to the heater and fuel, or at fuel failure (defined by the experimenters as the downward movement of the upper electrode by >1.0 mm) Typically in the I-series tests this fuel failure is accompanied by a gross increase in the diameter of the fuel pellets, by molten fuel squirting through a crack in the quartz container, or by a sequence of diametral increase and squirting. The primary objective of the experiments is to determine the influence of the transient history on these failure modes.

The IC-series tests [4] were run using fuel pin samples with their stainless steel cladding intact. The external heater was used to melt the cladding prior to increasing the electric current through the sample. The tests analyzed here are IC-2, IC-30, and IC-29 which used low burnup HEDL N-E fuel (2.5 at.% burnup,

40 kW/m), medium burnup PNL-9 fuel (4.7 at.%, 18 kW/m), and high burnup PNL-7 fuel (9.9 at.%, 26 kW/m), respectively. All of these tests were terminated after the cladding meltoff phase.

F-series TREAT Tests

The F-series tests [2] are performed in dry (no sodium) capsules in the TREAT reactor to study fuel behavior under LOF conditions. The most recent tests in this series were F3 and F4. These experiments were designed to study the timing and mode of fuel disruption under greater than nominal power levels. Sample power was increased on a 200-ms period until constant powers of 82.0 and 216.5 kW/m were achieved in F3 and F4, respectively. Nominal power and burnup for the PNL-7 fuel used in F3 and F4 were 29.5 kW/m and 9 at.%.

The principal instrumentation in the F3 and F4 tests was a high-speed photographic system. The TREAT fast neutron hodoscope was also used to monitor fuel motion.

Fission Gas Release Tests

The HEDL FGR apparatus [5] consists of an in-cell, continuously evacuated chamber containing the test fuel in a sealed tungsten heater/capsule. The tungsten is heated by an electric current, providing an external source of heat to the test fuel. In contrast to the DEH tests, this external heater is the sole source of heat. The gases evolving from the test fuel are contained within the tungsten capsule and continuously sampled to determine the gas composition and the partial pressures of the components. The quantity of fission gas released can then be calculated yielding a fractional release as a function of time. Visual information is available only on the final condition of the fuel; difficulties were encountered in observing time-dependent gross disruption, and these data are not reported. The time-dependent temperature profile in the test fuel is calculated from the measured capsule temperature with a maximum expected error of ± 150 K.

The FGR tests analyzed here are experiments 40, 41, and 44 through 52. The fuel elements used in these tests are from the PNL-10 subassembly irradiated in EBR-II to 4.45 at.% burnup at a peak power of 24.4 kW/m. The elements were sectioned for pretest characterization and for the actual tests. The cladding associated with each section was left intact to avoid disturbing the fuel within. (During the experiments, the cladding is melted off by the heater. Provisions were made to permit the molten cladding to flow away from the fuel into a small well, allowing unobstructed radiative heat transfer between the heater and the fuel.)

In general, the FGR tests listed above are conducted in pairs to examine the effects of varying a single parameter. In five of the eleven tests the heating simulates the initiating phase of a loss-of-flow accident in a breeder reactor. As described for the DEH tests, these simulations begin with a slow heating ramp followed by a second, more rapid ramp. In one case (FGR 52), an attempt was made to impose a third ramp simulating a power burst in the reactor, but limits on the capsule temperature did not allow the high rates necessary for a realistic simulation.

In none of the FGR tests considered in this study did the fuel temperatures reach the melting point and in most cases the pellets remained intact. The intact fuel permitted extensive posttest examination yielding detailed information on gas bubble size and distribution and on changes in the fuel microstructure and gross dimensions.

RESULTS

The entire results from the comparison of model predictions with the fuel disruption experiments are too extensive to be presented here. Representative results will be given instead. For this purpose the FGR tests are best suited for the FRAS3 comparison because these experiments provide the most detailed information on fission gas behavior. On the other hand, the DEH and F series tests, along with the FGR tests, can all be compared with the D-D model since the D-D model is primarily concerned with gross fuel behavior.

Comparison of FRAS3 with the FGR Experiments

FRAS3 calculations were compared with measured fuel diameter increases, local porosity changes, time-dependent fission gas release, and final bubble distributions. In all of these comparisons the feedback between the fission gas behavior and the fuel mechanical response was ignored. Not surprisingly therefore, only weak agreement was found between calculated swelling and measured fuel diameter increases. Better agreement was found between calculated local swelling and measured porosity changes. As seen in Table I, there is good qualitative agreement (the tests are correctly ordered by increasing porosity change), but the quantitative agreement is somewhat weak with FRAS3 consistently overpredicting the swelling. Part of this disagreement is undoubtedly due to the neglect of the compressive stresses that swelling causes in the fuel. Another source of error is the assumption that grain boundary bubbles equilibrate instantaneously upon coalescence. The new grain boundary bubble equilibration model that has recently been incorporated into FRAS3 [7,8] eliminates this deficiency.

TABLE I

Local Porosity Changes in FGR Tests[1]

Test	FRAS3 Predicted Change Total (%)	Grain Face & Grain Edge (%)	Measured Change (%)
46	3.8	1	0
50	38	6	8
48	38	7	12
45	46	10	18
44	61	9	32
52	64	20	46
41	84	13	58

[1]All results at 0.9 R_F, where R_F = 2.47 mm is the nominal outer fuel radius.

Figures 1 and 2 compare measured fractional gas release and FRAS3 calculated gas release at 0.9 R_F for two different FGR tests. Other calculations for different tests and using different unrestructured fuel nodes gave similar results. In some cases the total gas release was overpredicted while in other cases the total gas release was underpredicted. Additional FRAS3 calculations showed that the predicted total gas release could usually be brought into agreement with the experiments by varying the temperature and initial gas concentration within the experimental error. A persistent source of disagreement, however, was found between the measured and calculated time of initial gas release. A definite pattern was noted in this disagreement. The calculated time of initial gas release

for tests that were begun immediately with a fast temperature ramp, such as FGR 45 shown in Fig. 1, was always later than the measured time. On the other hand, there was excellent agreement between calculated and measured time of initial gas release for tests that started with an extended slow ramp prior to the final fast ramp. One such test was in FGR 50, shown in Fig. 2. It was concluded that this pattern may be due to the FRAS3 initial conditions. It is assumed in the version of the code used here that all fission gas retained from the pretransient irradiation is in solution within the fuel grains, so that no gas is initially distributed in intragranular bubbles or on the grain faces or edges. On the other hand, measurements have shown that 20-25% of the retained gas is in fact located intergranularly in the FGR test fuel. One can conjecture, therefore, that in tests such as FGR 50, the test conditions permitted the code to redistribute some of the gas to the grain faces, in effect establishing more realistic boundary conditions for the rapid conditions. In the case of an single fast ramp there is less opportunity to redistribute the gas, causing an error in the predicted onset of gas release. In order to investigate this further, FRAS3 has recently been modified to allow an initial grain boundary bubble distribution to be input into the code.

FRAS3-calculated and measured intragranular bubble-size distributions for tests FGR 45 and FGR 50 are shown in Figs. 3 and 4, respectively. The numbers on the experimental curves in these figures give the distance from the outer fuel radius R_F (~2.47 mm) at which the measurements were taken. With exceptions, when all of the experiments were considered, a trend was seen in which FRAS3 underestimates the percentage of smaller bubbles in the grains, while correctly estimating the upper limits of the bubble diameter distribution. That is, because the figures show the cumulative percentage of bubbles smaller than a given size, the convergence of the data and calculational results at the right-hand side of the figures indicates that the code is correctly predicting the probable maximum bubble size. This convergence does not mean that the code is correctly predicting the diameter probability density function, the measure of the relative number of bubbles of each size. This function is found from the slope of the lines. Thus, in Figs. 3 and 4 the code underestimates the percentage of bubbles between ~ 40 nm and ~ 60 nm (data plots tend to rise more sharply than predicted), correctly estimates the percentage of bubbles between ~ 60 nm and ~150 nm (slopes are approximately the same), and overestimates the percentage of large bubbles (data plots rise less sharply than predicted).

Comparison of the D-D Model with Experiments

Calculations [9] of earlier DEH and FGR experiments using the D-D model have shown excellent agreement. The calculations reported below generally support that agreement. It was necessary, however, to recalibrate the model since the DEH experimenters have corrected their temperature calculations for tests I-28, I-30, and I-43, all of which were used to calibrate the model.

Table II compares calculated swelling threshold time using the D-D model with the observed swelling behavior for 23 DEH and FGR tests. Because the time at which swelling began in these experiments was generally not reported, it was necessary here to make a weaker comparison of the calculated swelling threshold with the test duration time (defined as the ramp length for single ramp tests and the final ramp length for double ramp tests). If the test duration is less than the swelling threshold, swelling behavior is not predicted. If the test duration is greater than the swelling threshold, swelling is predicted. The last two columns of Table II compare predicted and observed swelling behavior. There is disagreement in only four of the experiments and the difference in swelling threshold time and test duration for these four experiments is so small that the results could easily be made to agree by changing the fuel temperatures within the experiment error.

As noted previously, the D-D model has recently been extended [10] to quantify observed fuel fragmentation behavior in DEH-IC series tests on stainless steel clad samples. In some tests on fuel with high burnup, significant fuel spallation was reported [4] at the onset of cladding melting. These experiments have been analyzed with the D-D model by assuming that fission-gas bubbles on grain boundaries are subjected to a compressive constraining force maintained by intact cladding. When the constraining force is removed at cladding failure, the bubbles are overpressured and may fracture the grain boundaries. In the preliminary analysis of fuel fragmentation, a constraining pressure of 4 MPa was chosen as being representative of the cladding strength at elevated temperature. Comparison of calculations with particle size and velocity measured in DEH tests IC-2, 29, and 30 showed good agreement [10]. Later DEH-IC tests indicated that cesium vapor may play a role in fuel spalling and fragmentation. One explanation for this behavior which has been investigated here is that the vapor pressure of cesium in the fuel cladding gap may provide the compressive force between the fuel and cladding. Relief of this force causes the fuel to fracture. Calculations of cladding failure show that cesium vapor will fail the cladding near the cladding melting point and that the pressure is about 4-5 MPa. Such a pressure is also consistent with the pressure on the cladding that would be necessary to cause the observed [4] unstable growth of helium bubbles in the cladding during terminated DEH tests.

Concurrent with the DEH-IC tests, a set of two in-reactor F-series TREAT tests were also executed to look at disruption of high burnup fuel under LOF conditions. Tests F3 and F4 [2] used the same high burnup PNL-7 that had shown the maximum spallation in the DEH-IC tests. The camera was set up to follow a sequence of cladding melting, limited solid fuel spallation, fuel swelling, fuel melting, and eventually complete disruption of the pin geometry. However, in both tests the fuel completely disrupted well before fuel melting, or even complete cladding melting, occurred. In the case of F3 the maximum cladding temperature was calculated to be 1427°C with 41% melt fraction while in F4 the cladding reached only 1233°C. The observed disruption was so vigorous and so complete that from one film frame to the next, 1-2 ms later, the entire sample appears to have fragmented.

Application of the D-D model to tests F3 and F4 shows that the effect of cladding constraint on fission gas bubble behavior can also explain the results of these tests. A constraining pressure of 4-5 MPa is consistent with both the observed cladding failure time and the observed fragmentation. Again, one source for this pressure is volatile fission products in the fuel-cladding gap.

Discussion and Conclusions

In general the FRAS3 calculations showed reasonable agreement with measured porosity changes, time-dependent gas release, and bubble-size distributions in the FGR tests analyzed. The comparison of FRAS3 with the experiments has led to recent improvements in the code which now includes a grain-boundary bubble equilibration model and a capability for inputing an initial bubble distribution into the code. In addition, a multi-node version of FRAS3 is being coupled to the FPIN fuel pin mechanics code to investigate the effects of feedback between fission gas swelling and stresses in the fuel.

The DiMelfi-Deitrich (D-D) model has been shown to accurately predict the gross behavior (swelling vs. non-swelling) of recent FGR and DEH tests. An extension of the D-D model to include a quantitative assessment of fuel fragmentation has been found to explain both the fuel spallation observed in the DEH-IC series tests and the vigorous fuel disruption observed in the F3 and F4 TREAT tests. Volatile fission products such as cesium in the fuel-cladding gap may play a role in this fragmentation by providing the constraining pressure on the fuel prior to cladding melting.
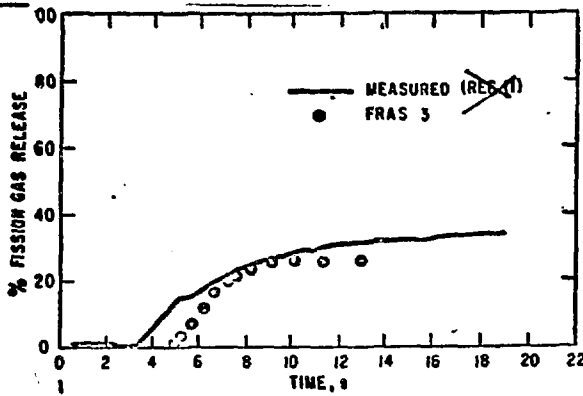
FIG. 1. Fission gas release for FGR 45
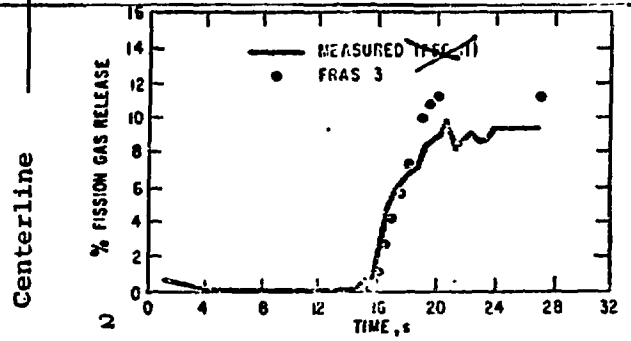
FIG. 2 Fission gas release for FGR 5
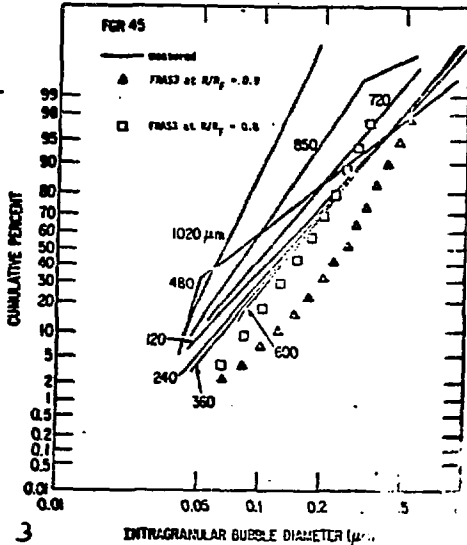
LLUSTRATION

FIG. 3 BUBBLE-SIZE Distribution for FGR 45
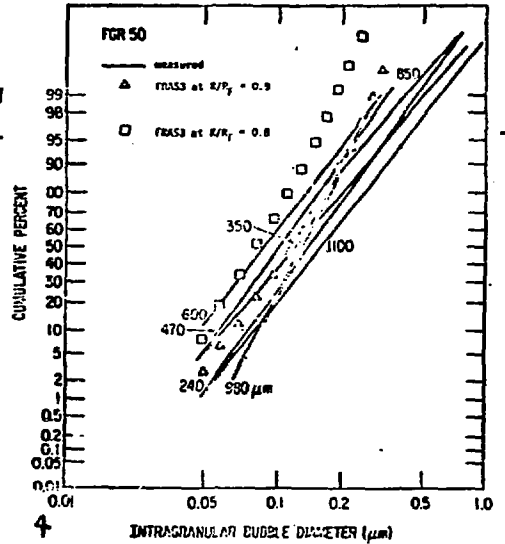
FIG. 4 BUBBLE-SIZE DISTRIBUTION FOR FGR 50

Centerline

TABLE II

D-D MODEL PREDICTIONS VS. OBSERVATIONS IN DEH AND FGR TESTS[1]

Test	Initial Temp (K)	Initial Ramp Rate (K/s)	Initial Ramp Length (s)	Final Ramp Rate (K/s)	Final Ramp Length (s)	Predicted Swelling Threshold (s)	Swelling Predicted	Swelling Observed
DEH								
I-35	1361	36	9.9	-	-	27.5	no	no
I-37	1333	80	7.3	649	1.3	0.7	yes	yes
I-38	1579	41	4.6	206	0.7	2.0	no	no
I-39	1403	34	7.0	580	1.3	1.1	yes	yes no
I-40	1526	24	16.7	478	0.9	0.9	yes	yes
I-41	1538	27	14.0	-	-	30.2	no	no
I-42	1530	26	17.4	343	0.4	1.0	no	no
I-43	1538	23	23.1	262	1.7	1.0	yes	yes
I-44	1021	38	7.9	487	1.8	1.3	yes	yes
I-45	1445	700	2.4	-	-	2.3	yes	no
I-48	1526	464	3.6	-	-	3.0	yes	yes
I-49	1418	708	2.6	-	-	2.3	yes	yes
FGR								
40	1623	160	10.0	-	-	7.1	yes	yes
41	1523	150	8.0	-	-	8.0	yes	yes
44	1483	127	7.4	-	-	9.3	no	no
45	1483	400	2.0	-	-	3.6	no	no
46	1293	20	21.0	-	-	49.1	no	no
47	1453	23	21.0	-	-	38.7	no	no
48	1503	32	5.0	170	5.0	4.8	yes	no
49	1239	30	26.0	110	4.0	4.6	no	no
50	1419	16	11.0	140	6.0	5.9	yes	no
51	1493	15	10.0	160	10.0	5.1	yes	yes
52	1433	16	15.0	120	9.0	6.2	yes	yes

END.

[1]DEH results at 0.9 R_F. FGR results at 0.8 R_F.

REFERENCES

1. L. W. Deitrich, "An Assessment of Early Fuel Dispersal in the Hypothetical Loss-of-Flow Accident," *Proceedings of the International Meeting on Fast Reactor Safety Technology,* ANS-ENS, Seattle (1979), p. 615.

2. R. G. Palm, "TREAT F-series LMFBR Loss-of-Flow Experiments," *Conference on Fast, Thermal, and Fusion Reactor Experiments,* ANS, Salt Lake City, Utah (1982).

3. G. Bandyopadhyay and J. A. Buzzell, "Role of Fission Gas and Fuel Melting in Fuel Response During Simulated Hypothetical Loss-of-Flow Transients," *Nucl. Tech.,* 47, 91 (1980).

4. G. R. Fenske and G. Bandyopadhyay, "The Effect of Burnup on the Response of Stainless-Steel-Clad Mixed-Oxide Fuels to Simulated Thermal Transients," *J. Am. Ceram. Soc.,* 64, 375 (1981).

5. C. A. Hinman and E. H. Randklev, "Transient Redistrubution of Intragranular Fission Gas in Irradiated Mixed Oxide," *ANS/ENS Topical Meeting on Reactor Safety Aspects of Fuel Behavior,* Sun Valley, Idaho (1981), p. 2-247.

6. E. E. Gruber and E. H. Randklev, "Comparison of Fission-Gas Effects in a Transient Overpower Test (HUT5-7A) to FRAS3 Code Predictions," *Proceedings of the International Meeting on Fast Reactor Safety Technology,* ANS/ENS, Seattle (1979), p. 2050.

7. E. E. Gruber, "Transient Fission-Gas Swelling Due to Grain-Boundary Bubble Growth," *Trans. Am. Nucl. Soc.,* 38, 371 (1980).

8. E. E. Gruber, "Diffusional Growth of Overpressured Fission-Gas Bubbles on Grain Boundaries," *J. Nucl. Materials* (submitted for publication).

9. R. J. DiMelfi and L. W. Deitrich, "The Effects of Grain Boundary Fission Gas on Transient Fuel Behavior," *Nucl. Tech.,* 43, 328 (1979).

10. R. D. DiMelfi and G. R. Fenske, "Modeling Solid-Fuel Dispersal During Slow Loss-of-Flow-Type Transients," *Transactions of the 6th International Conference on Structural Mechanics in Reactor Technology,* C1/1, (1981).

DISCLAIMER